Polymer 54 (2013) 155–161

Contents lists available at SciVerse ScienceDirect

Polymer

journal homepage: www.elsevier.com/locate/polymer

Benzooxadiazole-based donor/acceptor copolymers imparting bulk-heterojunction solar cells with high open-circuit voltages

Jian-Ming Jiang, Po-An Yang, Shang-Che Lan, Chia-Ming Yu, Kung-Hwa Wei*

Department of Materials Science and Engineering, National Chiao Tung University, 300 Hsinchu, Taiwan

ARTICLE INFO

Article history:
Received 21 August 2012
Received in revised form
2 November 2012
Accepted 14 November 2012
Available online 20 November 2012

Keywords:
Polymer solar cell
Suzuki coupling
Donor/acceptor conjugated polymers

ABSTRACT

In this study we used Suzuki cross-coupling to synthesize three new donor/acceptor copolymers—**PFTBO**, **PAFTBO**, and **PCTBO**—featuring soluble alkoxy-modified 2,1,3-benzooxadiazole (**BO**) moieties as acceptor units and electron-rich building blocks—dialkyl fluorene (**F**), alkylidene fluorene (**AF**), and carbazole (**C**), respectively—as donor units. These polymers, which we characterized using gel permeation chromatography, thermogravimetric analysis, NMR spectroscopy, UV–Vis absorption spectroscopy, and electrochemical cyclic voltammetry, exhibited good solubility, low-lying energy levels for their highest occupied molecular orbitals, excellent thermal stability, and air stability. Using these polymers, we fabricated bulk-heterojunction solar cell devices having the structure indium tin oxide/poly(3,4-ethylenedioxythiophene):polystyrenesulfonate/polymer:[6,6]-phenyl-C_{61}-butyric acid methyl ester ($PC_{61}BM$) (1:1, w/w)/Ca/Al. Under AM 1.5G illumination (100 mW cm^{-2}), the solar cell incorporating **PFTBO** exhibited a high value of V_{oc} of 1.04 V and that based on **PCTBO** provided a power conversion efficiency of 4.1% without the need for any post treatment.

1. Introduction

Polymer solar cells (PSCs) are attracting growing interest as a potential renewable energy technology because they can be manufactured at low cost with the capability of being used in flexible large-area devices [1–3]. To date, bulk-heterojunctions (BHJs), in which the active layer consists of a blend of electron-donating conjugated polymers and electron-accepting fullerene derivatives, have been the most prevalent active layer structures in polymer solar cells exhibiting high power conversion efficiencies (PCEs). Several conjugated polymers have been developed featuring electron donor/acceptor (D/A) units in main chain–conjugated configurations [4–15] and side chain–attached architectures [16–20]. Recently, BHJ solar cells based on blends of some D/A low-band gap polymers and [6,6]-phenyl-C_{61}-butyric acid methyl ester ($PC_{61}BM$) or $PC_{71}BM$ have been investigated extensively, providing PCEs as high as 7% [21–27].

The PCE of a solar cell device is essentially determined by short-circuit current density (J_{sc}), the fill factor, and the open-circuit voltage (V_{oc}). The relatively low open-circuit voltage (ca. 0.6 V) obtained in some thiophene-polymer based BHJ devices will limit their PCEs. In a BHJ-structured active layer, the open-circuit voltage is typically proportional to the difference in energy between the highest occupied molecular orbital (HOMO) of the polymer and the lowest unoccupied molecular orbital (LUMO) of the fullerene, although some other characteristics of the device structure (e.g., the type of cathode material, the active layer morphology, or exciton non-radiative recombination) can also affect the values of V_{oc} of BHJ PSCs [28–31]. Therefore, the value of V_{oc} can be increased either by elevating the LUMO energy level of the fullerene or depressing the HOMO energy level of the polymer while keeping its counterpart unchanged. Low-band gap polymers that provide efficient absorption of the solar spectrum, however, tend to have high-lying HOMOs and low-lying LUMOs; the difference in the energy levels between the low-lying LUMOs of the polymers and the LUMO of the fullerene frequently result in inefficient charge separation, leading to a smaller enhancement of J_{sc}. On the other hand, the combination of a high-lying HOMO in a low-band gap polymer and a fixed LUMO in fullerene will also provide a lower value of V_{oc}. Therefore, fine tuning of the band gap and the energy levels such as lowering the HOMO and LUMO of the polymer simultaneously but with a larger decrease in the LUMO while maintaining its value 0.3 eV above that of the fullerene is required to obtain BHJ PSCs with high values of V_{oc} and J_{sc} [32–34]. Currently, the highest open-circuit voltages obtained from BHJ PSCs (ca. 1 V) have required polymers possessing medium-sized band gaps (ca. 2 eV) [35–38].

* Corresponding author.
E-mail address: khwei@mail.nctu.edu.tw (K.-H. Wei).

0032-3861/$ – see front matter © 2012 Elsevier Ltd. All rights reserved.
http://dx.doi.org/10.1016/j.polymer.2012.11.034

In recent years, 9,9-dialkylfluorenes have emerged as attractive donor candidates for D/A polymer photovoltaics because of their good processability, high absorption coefficients, and considerable values of V_{oc} [39,40]. By changing the sp^3-hybridized carbon atom at the 9-position of 9,9-dialkylfluorene to an sp^2-hybridized atom, the resulting alkylidene fluorene permits the alkyl chains to adopt a coplanar conformation relative to the polymer backbone, thereby facilitating cofacial π–π stacking, which can lead to very short intermolecular distances (<4 Å) in crystalline or liquid crystalline states and, accordingly, enhanced charge carrier transportation [41]. Unlike a C-bridged fluorene, the corresponding N-bridged carbazole moiety is fully aromatic, providing superior chemical and environmental stability. Poly(*N*-alkyl-2,7-carbazole) derivatives have been applied successfully in polymer light emitting diodes [42] and organic field-effect transistors [43], demonstrating good p-type transport properties.

On the other hand, BHJ devices based on main chain D/A polymers containing alkoxy benzooxadiazole (BO) units as acceptors and several thiophene-based building blocks as donors have exhibited relatively high values of V_{oc} [44,45]; therefore, combining a strongly electron-withdrawing acceptor with a weakly electron-donating donor can be a very effective means of lowering the HOMO energy level in the D/A polymer and, ultimately, enhancing the value of V_{oc} of the resulting PSC [46]. Those studies inspired us to further explore the possibility of copolymerizing alkoxy-modified BO derivatives with weakly electron-donating units to synthesize copolymers exhibiting high values of V_{oc}. In this study, we prepared a series of new D/A alternating polymers—**PFTBO**, **PAFTBO**, and **PCTBO**—based on 9,9-dialkylfluorene (**F**), alkylidene fluorene (**AF**), and *N*-alkyl-2,7-carbazole (**C**) units, respectively, as weak electron donors and alkoxy-modified BO (**BO**) units as electron-deficient acceptors; conjugation of the electron-withdrawing BO units to the weakly electron-donating units provided polymers with deep HOMO energy levels and medium-sized band gaps. These desirable features provided **PFTBO**, **PAFTBO**, and **PCTBO** with good hole mobilities and high values of V_{oc}, making them suitable for photovoltaic applications.

2. Experimental section

2.1. Materials and synthesis

The synthesis of 4,7-bis(5-bromothiophen-2-yl)-5,6-bisoctyloxybenzo[*c*][1,2,5]oxadiazole (**M1**) [44] has been reported elsewhere.

4,4,5,5-Tetramethyl-2-[2-(4,4,5,5-tetramethyl-1,3-dioxolan-2-yl)-9,9-dioctyl-9*H*-fluoren-7-yl]-1,3-dioxolane (**M2**) [47], 2-[9-(heptadecan-9-ylidene)-2-(4,4,5,5-tetramethyl-1,3-dioxolan-2-yl)-9*H*-fluoren-7-yl]-4,4,5,5-tetramethyl-1,3-dioxolane (**M3**) [41], and 9-(heptadecan-9-yl)-2,7-bis(4,4,5,5-tetramethyl-1,3-dioxolan-2-yl)-9*H*-carbazole (**M4**) [48] were prepared according to reported procedures. $PC_{61}BM$ was purchased from Nano-C. All other reagents were used as received without further purification, unless stated otherwise.

2.2. General procedure for Suzuki polymerization: alternating polymer PFTBO

A mixture of **M1** (105 mg, 0.150 mmol), **M2** (96.3 mg, 0.150 mmol), Aliquat 336 (ca. 20 mg), $K_2CO_{3(aq)}$ (2 M, 1.5 mL), and chlorobenzene (CB) 4 mL were degassed under N_2 at 60 °C for 15 min. $Pd(PPh_3)_4$ was added to the mixture, which was then heated at 130 °C for 48 h. Phenylboronic acid (49.9 mg, 0.300 mmol) was added and then the mixture was stirred 6 h. Subsequently, bromobenzene (0.03 mL, 0.3 mmol) was also added to the mixture, which was stirred for another 12 h. After cooling to room temperature, the solution was added dropwise into MeOH (100 mL). The crude polymer was collected, dissolved in $CHCl_3$, and reprecipitated from MeOH. The solid was washed with MeOH, acetone, and $CHCl_3$ in a Soxhlet apparatus. The $CHCl_3$ solution was concentrated and then added dropwise into MeOH. The precipitate was collected and dried under vacuum to give **PFTBO** (100 mg, 72%). ^{1}H NMR (300 MHz, $CDCl_3$): δ 8.54–8.31 (m, 2H), 8.05–7.88 (m, 2H), 7.80–7.55 (m, 6H), 4.25 (br, 4H), 2.41 (br, 4H), 1.78–1.25 (m, 48H), 0.91 (s, 12H). Anal. Calcd: C, 76.25; H, 8.68; N, 3.01. Found: C, 75.18; H, 8.55; N, 3.15.

2.2.1. Alternating polymer PAFTBO

Using a polymerization procedure similar to that described above for **PFTBO**, a mixture of **M1** (105 mg, 0.15 mmol) and **M3** (98.1 mg, 0.15 mmol) in dry CB (4 mL) was polymerized to give **PAFTBO** (71 mg, 52%). ^{1}H NMR (300 MHz, $CDCl_3$): δ 8.51–8.29 (m, 2H), 8.17–7.98 (m, 2H), 7.78–7.51 (m, 6H), 4.22 (br, 4H), 2.81 (br, 4H), 1.98–1.56 (m, 48H), 0.83 (s, 12H). Anal. Calcd: C, 76.55; H, 8.57; N, 2.98. Found: C, 74.98; H, 8.42; N, 2.77.

2.2.2. Alternating polymer PCTBO

Using a polymerization procedure similar to that described above for **PCTBO**, a mixture of **M1** (105 mg, 0.15 mmol) and **M4** (98.6 mg, 0.15 mmol) in dry CB (4 mL) was polymerized to give **PCTBO** (120 mg, 85%). ^{1}H NMR (300 MHz, $CDCl_3$): δ 8.85–8.57 (m, 2H), 8.06–7.83 (m, 2H), 7.68–7.42 (m, 6H), 4.32 (br, 4H), 3.98 (s, 1H), 2.13 (br, 4H), 1.67–1.28 (m, 48H), 0.91 (s, 12H). Anal. Calcd: C, 75.03; H, 8.64; N, 4.45. Found: C, 73.15; H, 8.47; N, 4.56.

2.3. Measurements and characterization

^{1}H NMR spectra were recorded using a Varian UNITY 300-MHz spectrometer. Thermogravimetric analysis (TGA) was performed using a TA Instruments Q500 apparatus; the thermal stabilities of the samples were determined under a N_2 atmosphere by measuring their weight losses while heating at a rate of 20 °C min^{-1}. Size exclusion chromatography (SEC) was performed using a Waters chromatography unit interfaced with a Waters 1515 differential refractometer; polystyrene was the standard; the temperature of the system was set at 45 °C; THF was the eluent. UV–Vis spectra of dilute samples (1×10^{-5} M) in dichlorobenzene (DCB) were recorded at room temperature (ca. 25 °C) using a Hitachi U-4100 spectrophotometer. Solid films for UV–Vis spectroscopic analysis were obtained by spin-coating the polymer solutions onto a quartz substrate. Cyclic voltammetry (CV) of the polymer films was performed using a BAS 100 electrochemical analyzer operated at a scan rate of 50 mV s^{-1}; the solvent was anhydrous MeCN, containing 0.1 M tetrabutylammonium hexafluorophosphate ($TBAPF_6$) as the supporting electrolyte. The potentials were measured against a Ag/Ag^+ (0.01 M $AgNO_3$) reference electrode; the ferrocene/ferrocenium ion (Fc/Fc^+) pair was used as the internal standard (0.09 V). The onset potentials were determined from the intersection of two tangents drawn at the rising and background currents of the cyclic voltammograms. HOMO and LUMO energy levels were estimated relative to the energy level of the ferrocene reference (4.8 eV below vacuum level). Topographic and phase images of the polymer/$PC_{61}BM$ films (surface area: 5×5 μm^2) were obtained using a Digital Nanoscope III atomic force microscope (AFM) operated in the tapping mode under ambient conditions. The thickness of the active layer of the device was measured using a Veeco Dektak 150 surface profiler.

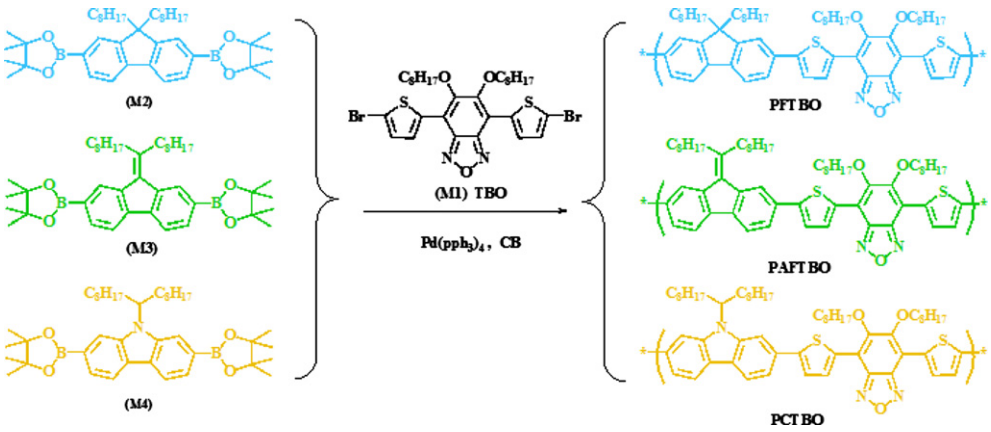

Scheme 1. Synthesis and structures of the polymers **PFTBO**, **PAFTBO**, and **PCTBO**.

2.4. Fabrication and characterization of photovoltaic devices

Indium tin oxide (ITO)–coated glass substrates were cleaned sequentially in detergent, water, acetone, and isopropyl alcohol (ultrasonication; 20 min each) and then dried in an oven for 1 h; the substrates were then treated with UV ozone for 30 min prior to use. An aqueous solution of poly(ethylenedioxythiophene): polystyrenesulfonate (PEDOT:PSS, Baytron P VP AI 4083) was spin-coated (5000 rpm) onto the ITO substrates. After baking at 140 °C for 20 min in air, a thin layer (ca. 20 nm) of PEDOT:PSS was formed on the substrates; the PEDOT:PSS–on–ITO samples were transferred to a N_2-filled glove box. The polymer and $PC_{61}BM$ were co-dissolved in DCB at various weight ratios, but with a fixed total concentration (40 mg mL^{-1}). The blend solutions were stirred continuously for 12 h at 90 °C and then filtered through a PTFE filter (0.2 μm); the photoactive layers were obtained by spin-coating (600–2000 rpm, 60 s) the blend solutions onto the ITO/PEDOT:PSS surfaces. The thickness of each photoactive layer was approximately 85–120 nm. The devices were ready for measurement after thermal deposition (pressure: ca. 1×10^{-6} mbar) of a 20-nm-thick film of Ca, followed by a 100-nm-thick Al film as the cathode. The effective layer area of one cell was 0.04 cm^2. The current density–voltage (J–V) characteristics were measured using a Keithley 2400 source meter. The photocurrent was measured under simulated AM 1.5 G illumination at 100 mW cm^{-2} using a Xe lamp–based Newport 66902 150-W solar simulator. A calibrated Si photodiode with a KG-5 filter was employed to confirm the illumination intensity. External quantum efficiencies (EQEs) were measured using an SRF50 system (Optosolar, Germany). A calibrated mono-silicon diode exhibiting a response at 300–800 nm was used as a reference. For hole mobility measurements, hole-only devices were fabricated having the structure ITO/PEDOT:PSS/polymer/Au. The hole mobility (μ_h) was determined by fitting the dark J–V curve into the space-charge-limited current (SCLC) model [16], based on the equation

$$J = \frac{9}{8}\varepsilon_0\varepsilon_r\mu_h\frac{V^2}{L^3}$$

where ε_0 is the permittivity of free space, ε_r is the dielectric constant of the material, V is the voltage drop across the device, and L is the thickness of active layer.

3. Results and discussion

3.1. Synthesis and characterization of the polymers

Scheme 1 outlines our general synthetic strategy for obtaining the monomers and the polymers. To ensure good solubility of the BO derivative **M1**, we positioned two octyloxy chains on the BO ring, as in previous reports [44]; we synthesized **M2**, **M3**, and **M4** using reported methods [41,47,48]. We performed Suzuki–Miyaura–Schlüter polymerization of the monomers in a biphasic mixture of CB and aqueous K_2CO_3 with $Pd(PPh_3)_4$ as the catalyst precursor. After polymerization for 48 h, we added phenylboronic acid and then bromobenzene (after a further 12 h) to end-cap the polymer; capping of the termini is necessary to obtain stable conjugated polymers exhibiting high photovoltaic performance [49,50]. Accordingly, we obtained the polymers **PFTBO**, **PAFTBO**, and **PCTBO** as dark-red solids in yields of 50–82%. We determined the weight-average molecular weights (M_w) of these polymers

Table 1
Molecular weights, thermal properties, and hole mobilities of the polymers.

Polymer	M_w[a] (kDa)	M_n[a] (kDa)	PDI[a]	T_d[b] (°C)	Mobility ($cm^2\ V^{-1}\ s^{-1}$)
PFTBO	67.8	45.2	1.5	316	1.2×10^{-4}
PAFTBO	34.6	18.2	1.9	300	5.1×10^{-4}
PCTBO	64.8	46.3	1.4	300	6.9×10^{-4}

[a] Values of M_n, M_w and PDI of the polymers were determined through GPC (polystyrene standards; THF).
[b] The 5% weight-loss temperature in air.

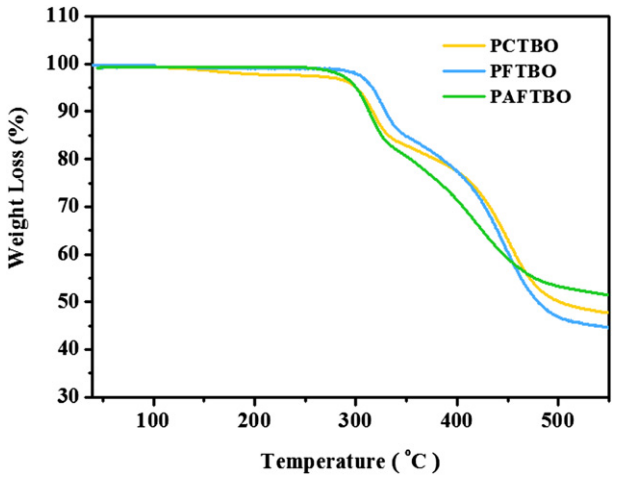

Fig. 1. TGA thermograms of the polymers **PFTBO**, **PAFTBO**, and **PCTBO**, recorded at a heating rate of 20 °C min^{-1} under a N_2 atmosphere.

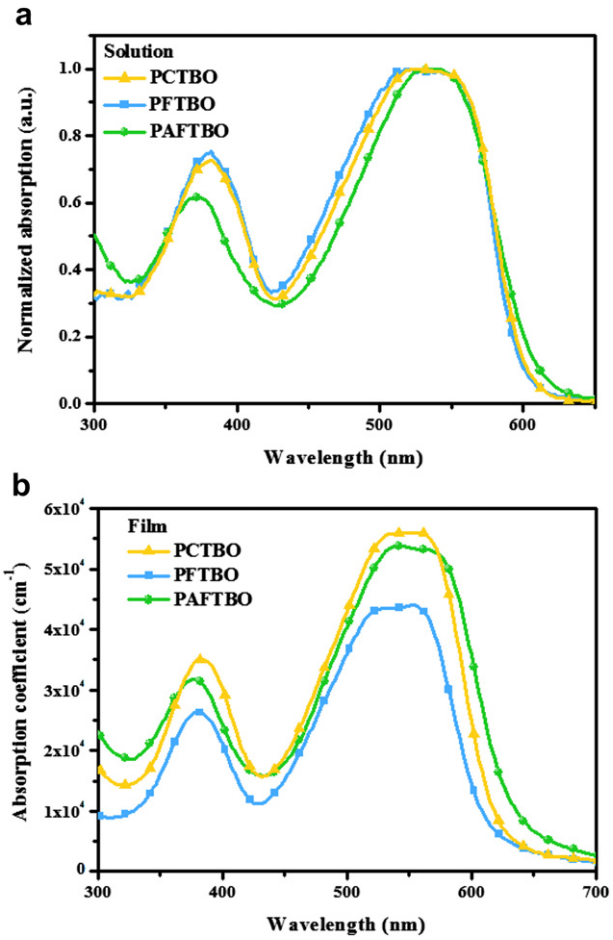

Fig. 2. UV–Vis absorption spectra of the polymers **PFTBO**, **PAFTBO**, and **PCTBO** as (a) dilute solutions in DCB (1×10^{-5} M) and (b) solid films.

(Table 1) through SEC, against polystyrene standards, in THF as the eluent.

3.2. Thermal stability

We used TGA to determine the thermal stability of the polymers (Fig. 1). In air, the 5% weight-loss temperatures (T_d) of **PFTBO**, **PAFTBO**, and **PCTBO** were 316, 300, and 300 °C, respectively. Thus, they all exhibited good thermal stability against O_2—an important characteristic for device fabrication and application. No clear glass transitions were evident from 25 to 300 °C in the DSC curves of the second heating and cooling runs (20 °C min^{-1}) of these polymers.

3.3. Optical properties

We recorded the normalized optical UV–Vis absorption spectra of the polymers as dilute DCB solutions at room temperature and as spin-coated films on quartz substrates. Fig. 2a displays the

Table 2
Optical properties of the polymers.

	$\lambda_{max,abs}$ (nm)		λ_{onset} (nm)	E_g^{opt} (eV)
	Solution	Film	Film	
PFTBO	525	540	630	1.96
PAFTBO	538	554	640	1.93
PCTBO	525	550	630	1.96

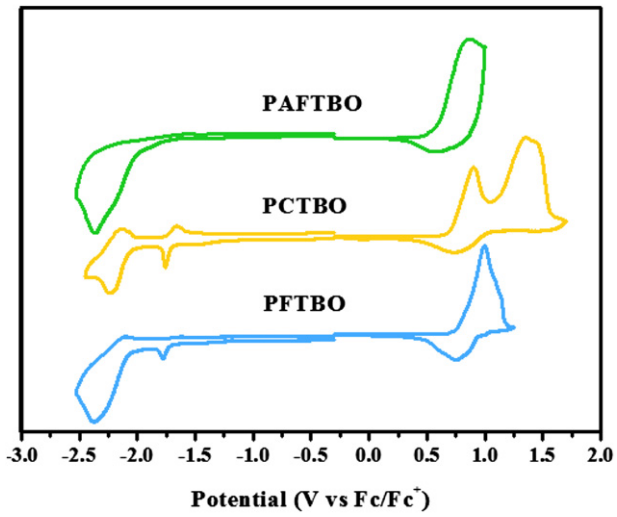

Fig. 3. Cyclic voltammograms of solid films of the polymers **PFTBO**, **PAFTBO**, and **PCTBO**.

Table 3
Electrochemical properties of the polymers.

	E_{onset}^{ox} (V)	E_{onset}^{red} (V)	HOMO[a] (eV)	LUMO[a] (eV)	E_g^{ec} (eV)
PFTBO	0.73	−1.69	−5.53	−3.11	2.42
PAFTBO	0.61	−1.73	−5.41	−3.07	2.34
PCTBO	0.70	−1.69	−5.50	−3.13	2.37

[a] HOMO and LUMO energy levels estimated from oxidation and reduction peaks, respectively, in cyclic voltammograms.

absorption spectra of **PFTBO**, **PAFTBO**, and **PCTBO** in DCB at room temperature; Table 2 summarizes the optical data, including the absorption peak wavelengths ($\lambda_{max,abs}$), absorption edge wavelengths ($\lambda_{edge,abs}$), and optical band gaps (E_g^{opt}). All of the absorption spectra recorded from dilute DCB solutions featured two absorption bands: one at 330–430 nm, which we assign to localized π–π* transitions, and another, broader band from 445 to 610 nm in the long wavelength region, corresponding to intramolecular charge transfer (ICT) between the acceptor (BO) and donor (9,9-dialkylfluorene, alkylidene fluorene, and *N*-alkyl-2,7-carbazole) units. The absorption spectra of the three polymers in the solid state were similar to their corresponding solution spectra, with slight red-shifts (ca. 20–40 nm) of their absorption maxima, indicating that some intermolecular interactions existed in the solid

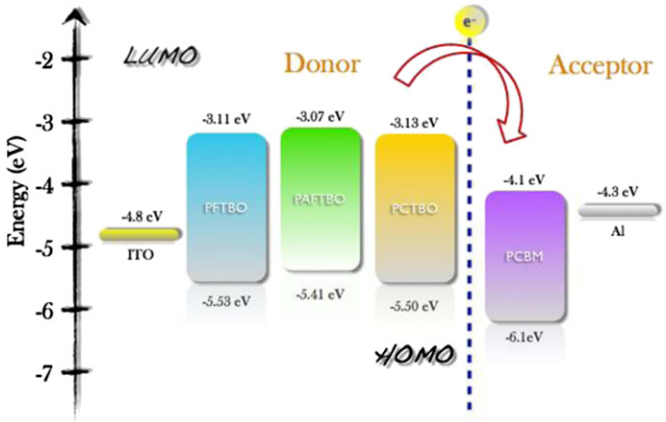

Fig. 4. Energy level diagram for **PFTBO**, **PAFTBO**, and **PCTBO**.

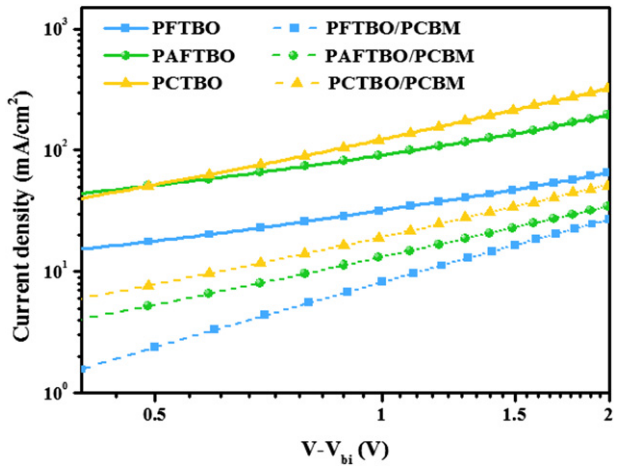

Fig. 5. Dark *J*–*V* curves for the hole-dominated carrier devices incorporating the pristine polymers and the blend films prepared at a blend ratio of 1:1 (w/w).

state. The absorption edges for **PFTBO**, **PAFTBO**, and **PCTBO** (Table 2) corresponded to optical band gaps (E_g^{opt}) of 1.96, 1.93, and 1.96 eV, respectively.

3.4. Electrochemical properties

Electrochemical cyclic voltammetry has been employed widely to investigate the redox behavior of polymers and to estimate their HOMO and LUMO energy levels. Fig. 3 displays the cyclic voltammograms of **PFTBO**, **PAFTBO**, and **PCTBO** films on a Pt electrode in a solution of $TBAPF_6$ (0.1 mol L^{-1}) in MeCN; Table 3 summarizes the relevant data. Irreversible n-doping/dedoping (reduction/re-oxidation) processes occurred for these polymers in the negative potential range—except for **PCTBO**, which underwent a partially reversible reduction. In addition, reversible p-doping/dedoping (oxidation/re-reduction) processes occurred in the positive potential range for each of these polymers. The onset oxidation potentials (E_{onset}^{ox}, vs. Ag/Ag^+) for **PFTBO**, **PAFTBO**, and **PCTBO** were 0.73, 0.61, and 0.70 V, respectively; their onset reduction potentials (E_{onset}^{red}) were −1.69, −1.73, and −1.69 V, respectively. On the basis of these onset potentials, we estimated the HOMO and LUMO energy levels according to the energy level of the ferrocene reference (4.8 eV below vacuum level) [51]. The HOMO energy levels of **PFTBO**, **PAFTBO**, and **PCTBO** were −5.53, −5.41, and −5.50 eV, respectively. The low-lying HOMO energy levels for these BO copolymers suggest that they are oxidatively stable hole-transporting materials [52,53]. In addition, low-lying HOMO energy levels are desirable for BHJ solar cells as an approach to maximize the values of V_{oc}. The LUMO energy levels of **PFTBO**, **PAFTBO**, and **PCTBO** were all located within a reasonable range (from −3.07 to −3.13 eV, Fig. 4) and were significantly greater than that of $PC_{61}BM$ (ca. −4.1 eV); therefore, we expected efficient charge transfer/dissociation to occur in their corresponding devices [54,55]. In addition, the electrochemical band gaps (E_g^{ec}) of **PFTBO**, **PAFTBO**, and **PCTBO**, estimated from the difference between the onset potentials for oxidation and reduction, were in the range 2.34–2.42 eV; that is, they were slightly greater than the corresponding optical band gaps (1.93–1.96 eV). The discrepancy between the electrochemical and optical band gaps presumably resulted from the exciton binding energies of the polymers and/or the interfacial barriers for charge injection [56].

Table 4
Photovoltaic properties of PSCs incorporating BO-based polymers.

Polymer/PC_{61}BM (1:1) (w/w)	V_{oc} (V)	J_{sc} (mA cm^{-2})	FF (%)	PCE (%)	Mobility (cm^2 V^{-1} s^{-1})	Thickness (nm)
PFTBO	1.04	5.4	47	2.6	3.1×10^{-5}	99
PAFTBO	0.97	7.1	50	3.4	8.7×10^{-5}	105
PCTBO	0.98	7.2	58	4.1	1.8×10^{-4}	101

3.5. Hole mobility

Fig. 5 displays the hole mobilities of devices incorporating the pristine polymers and the polymer/$PC_{61}BM$ blends at a blend ratio of 1:1 (w/w). The hole mobilities of the pristine **PFTBO**, **PAFTBO**, and **PCTBO** were 1.2×10^{-4}, 5.1×10^{-4}, and 6.9×10^{-4} cm^2 V^{-1} s^{-1}, respectively, while those of the **PFTBO**, **PAFTBO**, and **PCTBO** blends with $PC_{61}BM$ were 3.1×10^{-5}, 8.7×10^{-5}, and 1.8×10^{-4} cm^2 V^{-1} s^{-1}, respectively.

3.6. Photovoltaic properties

We investigated the photovoltaic properties of the polymers in BHJ solar cells having the sandwich structure ITO/PEDOT:PSS/polymer:$PC_{61}BM$ (1:1, w/w)/Ca/Al, with the photoactive layers having been spin-coated from DCB solutions of the polymer and $PC_{61}BM$. The optimized weight ratio for the polymer and $PC_{61}BM$ was 1:1.

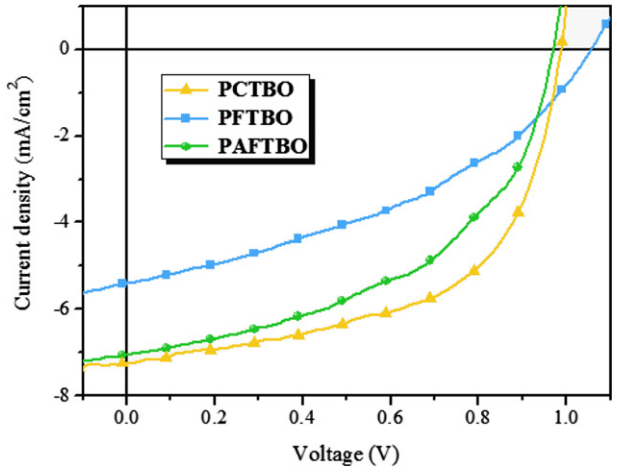

Fig. 6. *J*–*V* characteristics of PSCs incorporating polymer/$PC_{61}BM$ blends [blend ratio, 1:1 (w/w)].

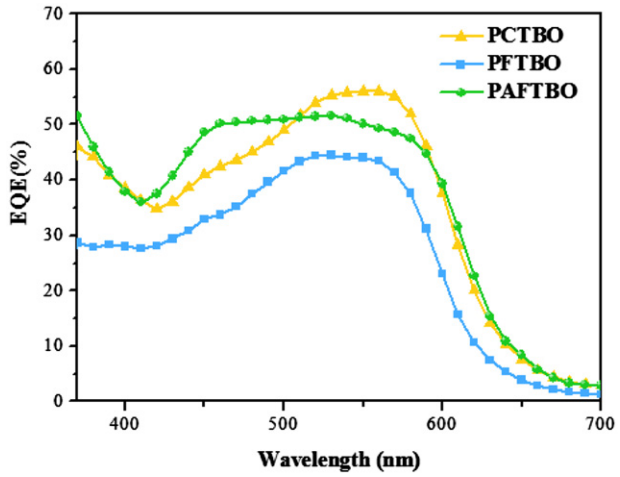

Fig. 7. EQE curves of PSCs incorporating polymer/$PC_{61}BM$ blends [blend ratio, 1:1 (w/w)].

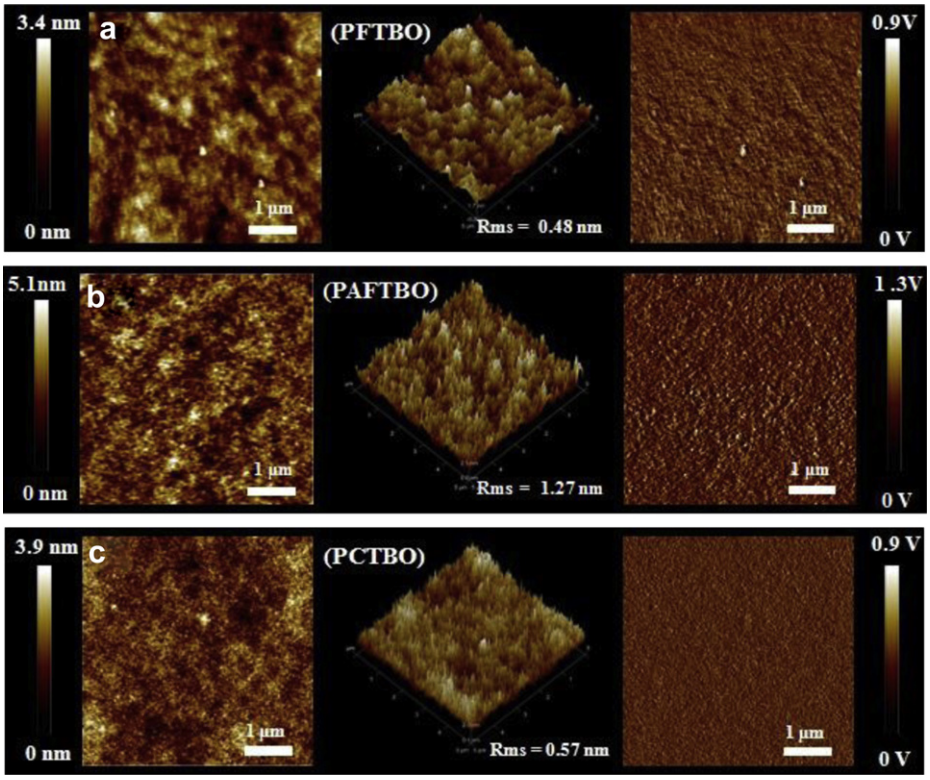

Fig. 8. Topographic AFM images of blends (1:1, w/w) of $PC_{61}BM$ with (a) **PFTBO**, (b) **PAFTBO**, and (c) **PCTBO**.

Fig. 6 presents the *J*–*V* curves of these PSCs; Table 4 summarizes the data. The devices prepared from the polymer/$PC_{61}BM$ blends of **PFTBO**, **PAFTBO**, and **PCTBO** exhibited high open-circuit voltages of 1.04, 0.97, and 0.98 V, respectively. Such high values of V_{oc} are consistent with these polymers having low-lying HOMO energy levels; notably, these open-circuit voltages are similar to the anticipated values. The short-circuit current densities of the devices incorporating **PFTBO**, **PAFTBO**, and **PCTBO** were 5.4, 7.1, and 7.2 mA cm^{-2}, respectively. Fig. 7 displays the EQE curves of the devices incorporating the polymer/$PC_{61}BM$ blends at weight ratios of 1:1. The theoretical short-circuit current densities obtained from integrating the EQE curves of the **PFTBO**, **PAFTBO**, and **PCTBO** blends were 5.2, 6.8, and 7.0 mA cm^{-2}—values that agree reasonably with the measured (AM 1.5 G) values of J_{sc}, with discrepancies of less than 5%. We attribute the higher values of J_{sc} of **PAFTBO** and **PCTBO** to their higher absorption coefficients (Fig. 2b); consistently, their EQE curve also featured higher responses at 400–650 nm. Therefore, more of the available photons from the solar radiation were absorbed by **PAFTBO** and **PCTBO**, leading to their devices exhibiting greater photocurrents.

The highest FF for the device incorporating **PCTBO**:$PC_{61}BM$ (1:1, w/w) as the active layer was likely due to the higher hole mobility of this active layer (Fig. 5); indeed, the hole mobilities of **PCTBO** and **PCTBO**:$PC_{61}BM$ (1:1, w/w) were greater than those of **PFTBO**, **PAFTBO**, **PFTBO**:$PC_{61}BM$ (1:1, w/w), and **PAFTBO**:$PC_{61}BM$ (1:1, w/w).

Moreover, when exploring the decisive factors affecting the efficiencies of PSCs, we must consider not only the absorption and energy levels of the polymers but also the surface morphologies of the polymer blends [57]. Fig. 8 displays the surface morphologies of our systems, determined using AFM. We prepared samples of the polymer/$PC_{61}BM$ blends using procedures identical to those employed to fabricate the active layers of the devices. In each case, we observed a quite smooth morphology for **PFTBO**, **PAFTBO** and **PCTBO** blend, with root-mean-square (rms) roughnesses of 0.48, 1.27, and 0.57 nm, respectively. The greater phase segregation and rougher surface of the **PAFTBO** blend presumably arose because of poor miscibility with $PC_{61}BM$; indeed, the solubility of **PAFTBO** was poorer than those of **PFTBO** and **PCTBO**.

A number of other factors can influence the efficiency of a device, including its molecular weight. For example, varying the number-average molecular weight (M_n) of PCDTBT from 10 to 22 kDa caused the PCEs of its devices to vary between 2.26 and 4.15% when using $PC_{61}BM$ as an acceptor; the 19-kDa polymer provided the best performance [58]. In our case, the value of M_n of **PAFTBO** was lower than those of **PFTBO** and **PCTBO**; we suspect that improving the solubility and the value of M_n of **PAFTBO** should result in PSCs exhibiting higher PCEs.

4. Conclusions

We have used Suzuki coupling polymerization to prepare a series of new conjugated polymers—**PFTBO**, **PAFTBO**, and **PCTBO**—featuring alternating 9,9-dialkylfluorene, alkylidene fluorene, and *N*-alkyl-2,7-carbazole units, respectively, as weakly electron-rich building blocks and TBO units as electron-deficient acceptors in their backbones. The open-circuit voltages of devices fabricated from **PFTBO**, **PAFTBO**, and **PCTBO** blended with $PC_{61}BM$ (weight ratio, 1:1) were 1.04, 0.97, and 0.98 V, respectively; these excellent values resulted from the relatively low HOMO energy levels of these polymers. The device incorporating **PCTBO** and $PC_{61}BM$ exhibited a high value of V_{oc} of 0.98 V, a value of J_{sc} of 7.2 mA cm^{-2}, a FF of 0.58, and a PCE of 4.1% without any post treatment.

Acknowledgment

We thank the National Science Council, Taiwan, for financial support (NSC 100-2120-M-009-006).

References

[1] Zhang S, Guo Y, Fan H, Liu Y, Chen HY, Yang G, et al. J Polym Sci Part A: Polym Chem 2009;47:5498.
[2] Wienk MM, Koon JM, Verhees WJH, Knol J, Hummelen JC, Vanhal PA, et al. Angew Chem Int Ed 2003;42:3371.
[3] Dennler G, Scharber MC, Brabec CJ. Adv Mater 2009;21:1323.
[4] Yuan MC, Chiu MY, Chiang CM, Wei KH. Macromolecules 2010;43:6270.
[5] Bijleveld JC, Gevaert VS, Nuzzo DD, Turbiez M, Mathijssen SGJ, Leeuw DM, et al. Adv Mater 2010;22:E242.
[6] Zhang Y, Hau SK, Yip HL, Sun Y, Acton O, Jen AKY. Chem Mater 2010;22:2696.
[7] Zhang Y, Zou J, Yip HL, Chen KS, Davies JA, Sun Y, et al. Macromolecules 2011; 44:4752.
[8] Jiang JM, Yang PA, Chen HC, Wei KH. Chem Commun 2011;47:8877.
[9] Dong Y, Cai WZ, Hu XW, Zhong CM, Huang F, Cao Y. Polymer 2012;53:1465.
[10] Wang XC, Luo H, Sun YP, Zhang MJ, Li XY, Yu G, et al. J Polym Sci Part A: Polym Chem 2012;50:371.
[11] Sun Y, Lin BP, Yang H, Gong XH. Polymer 2012;53:1535.
[12] Zhang J, Cai WZ, Huang F, Wang E, Zhong CM, Liu S, et al. Macromolecules 2011;44:894.
[13] Sun Y, Chien SC, Yip HL, Zhang Y, Chen KS, Zeigler DF, et al. J Mater Chem 2011;21:13247.
[14] Zhao W, Cai WZ, Xu RX, Yang W, Gong X, Wu HB, et al. Polymer 2010;51:3196.
[15] Wang XC, Sun YP, Chen S, Guo X, Zhang MJ, Li XY, et al. Macromolecules 2012; 45:1208.
[16] Wang HJ, Chen YP, Chen YC, Chen CP, Lee RH, Chan LH, et al. Polymer 2012;53: 4091.
[17] Duan C, Cai W, Huang F, Zhang J, Wang M, Yang TB, et al. Macromolecules 2010;43:5262.
[18] Huang F, Chen KS, Yip HL, Hau SK, Acton O, Zhang Y, et al. J Am Chem Soc 2009;131:13886.
[19] Zhang ZG, Liu YL, Yang Y, Hou K, Peng B, Zhau G, et al. Macromolecules 2010; 43:9376.
[20] Zhang ZG, Zhang S, Ming J, Chui CH, Zhang J, Zhang MJ, et al. Macromolecules 2012;45:113.
[21] Chen HY, Hou JH, Zhang SQ, Liang YY, Yang GW, Yang Y, et al. Nat Photonics 2009;3:649.
[22] Son HJ, Wang W, Xu T, Liang YY, Wu Y, Li G, et al. J Am Chem Soc 2011;133: 1885.
[23] Chu TY, Lu J, Beaupre S, Zhang Y, Pouliot JR, Wakim S, et al. J Am Chem Soc 2011;133:4250.
[24] Price SC, Stuart AC, Yang L, Zhou H, You W. J Am Chem Soc 2011;133:4625.
[25] Su MS, Kuo CY, Yuan MC, Jeng US, Su CJ, Wei KH. Adv Mater 2011;23:3315.
[26] Amb CM, Chen S, Graham KR, Subbiah J, Small C, So F, et al. J Am Chem Soc 2011;133:10062.
[27] Huo L, Zhang SQ, Guo X, Xu F, Li YF, Hou JH. Angew Chem Int Ed 2011;50: 9697.
[28] Brabed CJ, Cravino A, Meissner D, Sariciftci NS, Fromherz T, Rispens MT, et al. Adv Funct Mater 2001;11:374.
[29] He C, Zhong CM, Wu HB, Yang RQ, Yang W, Huang F, et al. J Mater Chem 2010; 20:2617.
[30] Vandewal K, Tvingstedt K, Gadisa A, Inganas O, Manca JV. Nat Mater 2009;8: 904.
[31] Blouin N, Michaud A, Gendron D, Wakim S, Blair E, Neagu PR, et al. J Am Chem Soc 2008;130:732.
[32] Chochos CL, Choulis SA. Polym Sci 2011;36:1326.
[33] Brabec CJ, Cowrisanker S, Halls JM, Laird D, Jia SJ, Williams SP. Adv Mater 2010;22:3839.
[34] Kirkpatrick J, Nielsen CB, Zhang W, Bronstein H, Ashraf RS, Heeney M, et al. Adv Energy Mater 2012;2:260.
[35] Du C, Li WW, Chen X, Bo ZH, Veit C, Ma ZF, et al. Macromolecules 2011;44: 7617.
[36] Qin RP, Li WW, Li CH, Du C, Veit C, Schleiermacher HF, et al. J Am Chem Soc 2009;131:14612.
[37] Uy RL, Price SC, You W. Macromol Rapid Commun 2012;33:1162.
[38] Sun JM, Zhu YX, Xu XF, Lan LF, Zhang LJ, Cai P, et al. J Phys Chem C 2012;116: 14188.
[39] Scherf U, List EJ. Adv Mater 2002;14:477.
[40] Fong HH, Papadimitratos A, Malliaras GG. Appl Phys Lett 2006;89:172116.
[41] Heeney M, Bailey C, Giles M, Shkunov M, Sparrowe D, Tierney S, et al. Macromolecules 2004;37:5250.
[42] Morin JF, Leclerc M, Ades D, Siove A. Macromol Rapid Commun 2005;26:761.
[43] Morin JF, Drolet N, Tao Y, Leclerc M. Chem Mater 2004;16:4619.
[44] Jiang JM, Yang PA, Hsieh TH, Wei KH. Macromolecules 2011;44:9155.
[45] Ding P, Zhong CM, Zou YP, Pan CY, Wu HB, Cao Y. J Phys Chem C 2011;115: 16211.
[46] Zhou HX, Yang L, Stoneking S, You W. Appl Mater Interfaces 2010;2:1377.
[47] Ranger M, Rondeau D, Leclerc M. Macromolecules 1997;30:7686.
[48] Blouin N, Michaud A, Leclerc M. Adv Mater 2007;19:2295.
[49] Kim Y, Cook S, Kirkpatrick J, Nelson J, Durrant JR, Bradley DDC, et al. J Phys Chem C 2007;111:8137.
[50] Heeger AJ, Park JK, Jo J, Seo JH, Moon JS, Park YD, et al. Adv Mater 2011;23: 2430.
[51] Pommerehne J, Vestweber H, Guss W, Mahrt RF, Bassler H, Porsch M, et al. Adv Mater 1995;7:551.
[52] Ong BS, Wu Y, Gardner S. J Am Chem Soc 2004;126:3378.
[53] Osaka I, Takimiya K, McCullough RD. Adv Mater 2010;22:4993.
[54] Thompson BC, Frechet JM. Angew Chem Int Ed 2008;47:58.
[55] Scharber MC, Muhlbacher D, Koppe M, Denk P, Waldauf C, Heeger AJ, et al. Adv Mater 2006;18:789.
[56] Wu PT, Kim FS, Champion RD, Jenekhe SA. Macromolecules 2008;41:7021.
[57] Chiu MY, Jeng US, Su MS, Wei KH. Macromolecules 2010;43:428.
[58] Waking S, Beaupre S, Blouin N, Aich BR, Rodman S, Gaudiana R, et al. Mater Chem 2009;19:5351.